Mon. Not. R. Astron. Soc. **000**, 1–**??** (2013)   Printed 12 March 2013   (MN LaTeX style file v2.2)

The S2 star as a probe of the accretion disk of Sgr A*

Dimitrios Giannios[1]⋆ and Lorenzo Sironi[2,3]†
[1]*Department of Physics, Purdue University, 525 Northwestern Avenue, West Lafayette, IN 47907, USA*
[2]*Harvard-Smithsonian Center for Astrophysics, 60 Garden St., Cambridge, MA 02138, USA*
[3]*NASA Einstein Postdoctoral Fellow*

arXiv:1303.2115v1 [astro-ph.HE] 8 Mar 2013

Received / Accepted

ABSTRACT
How accretion proceeds around the massive black hole in the Galactic center and other highly sub-Eddington accretors remains poorly understood. The orbit of the S2 star in the Galactic center passes through the accretion disk of the massive black hole and any observational signature from such interaction may be used as an accretion probe. Because of its early stellar type, S2 is expected to possess a fairly powerful wind. We show here that the ram pressure of the accretion disk shocks the stellar wind fairly close to the star. The shocked fluid reaches a temperature of $\sim 1\,$keV and cools efficiently through optically thin, thermal bremsstrahlung emission. The radiation from the shocked wind peaks around the epoch of the pericenter passage of the star at a luminosity potentially comparable to the quiescent emission detected from Sgr A*. Detection of shocked wind radiation can constrain the density of the accretion disk at a distance of several thousands of gravitational radii from the black hole.

Key words: accretion, accretion discs — black hole physics — galaxies: active — radiation mechanisms: thermal — shock waves — stars: winds, outflows

1 INTRODUCTION

The compact radio source Sgr A* is believed to mark the location of the massive black hole in the center of our Galaxy. The Galactic center is also observed as an IR and, possibly, X-ray source of luminosity $\sim 10^{36}$erg s^{-1} and $\lesssim 3\times10^{33}$erg s^{-1}, respectively (Genzel et al. 2010). Both IR (Ghez et al. 2004) and X-ray flaring (Baganoff et al. 2001) is regularly observed on timescales ranging from minutes to hours. Flares are believed to be associated with processes taking place close to the black-hole horizon.

The radiation observed from Sgr A* is believed to be powered by the accretion process. The radiative power is, however, a small fraction of the rate at which gravitational energy is released by the gas accretion. The accretion is, therefore, expected to take place through a hot, quasi-virialized, thick disk forming a "Radiatively Inefficient Accretion Flow" or RIAF. The fate of the non-radiated energy is model-dependent. The energy may be advected into the black hole through an "Advection-Dominated Accretion Flow" or ADAF (Narayan et al. 1995); carried by convective motions in a "Convection-Dominated Accretion Flow" or CDAF (Quataert & Gruzinov 2000; Ball et al. 2001); or in kinetic form through winds from the disk as in the "Inflow-Outflow Solutions" or ADIOS (Blandford & Begelman 1999, 2004). The various models make distinctly different predictions for the gas density and its radial profile in the disk, but convincing observational probes are still lacking. X-ray observations constrain the electron density close to the sphere of influence of the black hole (i.e., at the Bondi radius $R_{\rm b}\simeq 0.04$ pc $= 2\times10^5\,R_{\rm g}$, where $R_{\rm g} = GM_{\rm BH}/c^2$ is the gravitational radius for a black hole mass $M_{\rm BH} = 4.3\times10^6\,{\rm M}_\odot$) to be $n_{\rm b}\sim 100\,{\rm cm}^{-3}$ (Baganoff et al. 2003), but offer little clues for the gas properties within that radius, where the accretion disk is located.

The region of $R < R_{\rm b}$ is not devoid of sources (besides Sgr A*). It is filled with tens of massive stars, the so-called S cluster (Genzel et al. 2003; Gillessen et al. 2009). Most of these stars are B dwarfs and have elliptical orbits bringing them as close as $\sim$ a few$\times10^3\,R_{\rm g}$ from the black hole. B stars are also known to have powerful winds of substantial kinetic luminosities $L_w \gtrsim 10^{34}$ erg s^{-1} and characteristic mass loss rates of $\sim 10^{-7}\,{\rm M}_\odot$ yr^{-1}. Among the S-cluster stars, the S2 is characterized by both a close pericenter passage to Sgr A* and the earliest stellar type, possibly connected to the most powerful wind in the cluster. As we show here, the interaction of the wind of S2 with the accretion disk is expected to result in a characteristic rise of the X-ray emission from Sgr A* around the epoch of pericenter passage on a timescale of months, that can be used to probe the gas properties at the Galactic center.

2 THE S2 STAR AND THE ACCRETION DISK IN THE GALACTIC CENTER

The S2 star is the brightest of the S cluster. It has a ~16 year orbit around Sgr A* (Gillessen et al. 2009) of eccentricity $e = 0.88$ and a pericenter distance of $R_{\rm p} = 2800\,R_{\rm g}$. At pericenter, the velocity of the star reaches $v_{\rm p}\simeq\sqrt{2R_{\rm g}/R_{\rm p}}\,c\simeq 8\times10^8$ cm s^{-1}. The nature of

---

⋆ E-mail: dgiannio@purdue.edu (DG)
† E-mail: lsironi@cfa.harvard.edu (LS)

© 2013 RAS

the S2 star has been revealed in the study by Martins et al. (2008). S2 is an early B dwarf star (of spectral type B0-2.5V) of intrinsic luminosity $\log L/L_{\odot} = 4.2 \div 4.8$, effective temperature $T = (20 \div 30) \times 10^3$ K, and radius $R_* \simeq 10\,R_{\odot}$. The lack of particular wind absorption signatures in its spectrum places an upper limit on the wind mass loss rate of $\dot{M} \lesssim 3 \times 10^{-7} v_8$ $\mathrm{M_{\odot}}$ $\mathrm{yr^{-1}}$, where $v_w = 10^8 v_8$ cm $\mathrm{s^{-1}}$ is the speed of the wind.

The Martins et al. (2008) upper limit on the wind mass loss from S2 is only modestly constraining. Early B stars have, as a population, powerful and fast winds. Their wind velocity ranges within $v_w = (0.5 \div 2) \times 10^8$ cm $\mathrm{s^{-1}}$, while their mass loss rate is in the range $\dot{M} = (0.3 \div 3) \times 10^{-7}$ $\mathrm{M_{\odot}}$ $\mathrm{yr^{-1}}$ (Kudritzki & Puls 2000). Here we adopt $v_w = 10^8$ cm $\mathrm{s^{-1}}$ and $\dot{M} = 10^{-7}$ $\mathrm{M_{\odot}}$ $\mathrm{yr^{-1}}$ as reference values for the wind from S2, with the understanding that v_w is uncertain by a factor of ~ 2 and $\dot{M}$ by a factor of ~ 3.

The accretion rate of Sgr A* is quite uncertain and may well be distance-dependent. Theoretical modeling and Faraday rotation measurements place limits in the range $\dot{M}_{\rm BH} = 3 \times 10^{-9} \div 10^{-7}$ $\mathrm{M_{\odot}}$ $\mathrm{yr^{-1}}$ for the accretion rate at the black hole (Yuan et al. 2003; Marrone et al. 2007; Mościbrodzka et al. 2009). Given the estimated accretion rate, a radiatively efficient disk would radiate away $L \sim 0.1\dot{M}_{\rm BH}c^2 > 10^{37}$ erg $\mathrm{s^{-1}}$. The bolometric luminosity from Sgr A* is $\sim 10^{36}$ erg $\mathrm{s^{-1}}$ (Ghez et al. 2004) suggesting that the most of the gravitational energy released is likely not radiated away. Such an accretion flow is termed as RIAF. RIAFs are characterized by a thick $H/R \sim 1$ disk that is partially pressure and partially rotation supported. The total pressure (sum of the ram and gas pressures) of the disk at distance R from the black hole is $P \sim \rho c^2 (R_{\rm g}/R)$, where $\rho(R)$ is the gas mass density. This expression holds rather independently of the details of the adopted model for the flow (ADAF, CDAF, or ADIOS). The electron density at the Bondi radius $R_{\rm b} \sim 2 \times 10^5 R_{\rm g}$ is constrained directly by X-ray observations to be $n_{\rm b} \sim 100$ $\mathrm{cm^{-3}}$ (Baganoff et al. 2003). The gas density closer to the black hole is essentially unconstrained. Possible scalings for the density profile adopted here are $n = n_{\rm b}(R_{\rm b}/R)^{3/2}$ as, e.g., motivated by the ADAF solution (Narayan et al. 1995); or $n = n_{\rm b}(R_{\rm b}/R)$ as, e.g., motivated by GRMHD simulations (McKinney et al. 2012; Tchekhovskoy & McKinney 2012; Narayan et al. 2012). In the case of a CDAF, the density profile is shallower $n \propto R^{-1/2}$ (Quataert & Gruzinov 2000). At the pericenter of S2 (i.e., $R = R_{\rm p} \sim 0.01 R_{\rm b}$), the density of the disk material is, therefore, expected to be $n \sim n_{\rm b}(R_{\rm b}/R_{\rm p})^{1/2 \div 3/2} \sim 10^3 \div 10^5 \mathrm{cm^{-3}}$.

3 THE STELLAR WIND INTERACTION WITH THE ACCRETION DISK

The interaction of the stellar wind with the accretion disk has two potential observational signatures. The stellar wind is terminated by a strong shock because of the confining pressure of the disk. The shocked gas reaches a temperature of ~ 1 keV and cools via thermal bremsstrahlung emission mainly in the X-ray band. The RIAF also undergoes a shock upon interaction with the stellar wind. The shock may accelerate non-thermal particles (Narayan et al. 2012; Sadowski et al. 2013). Inverse Compton scattering of the bright stellar photon field by energetic electrons can power detectable hard X-ray and γ-ray emission.

3.1 Thermal emission from the shocked wind

While the stellar wind expands, its ram pressure drops with distance as $P_w = \dot{M} v_w / 4\pi r^2$, where lower case r is measured from the center of the star. The stellar wind is terminated by a strong shock at a distance $r_{\rm sh}$ where the wind ram pressure is balanced by that of the RIAF. The pressure of the RIAF is the sum of the thermal pressure and the ram pressure resulting from the relative motion of the RIAF and the star. The thermal pressure is of order $P_{\rm th} \sim \rho c^2 (R_{\rm g}/2R)$ while the ram pressure is mainly a result of the stellar motion, so that $P_{\rm ram} \sim 2\rho c^2 (R_{\rm g}/R)$. The ram pressure varies by $\sim 50\%$ depending on the angle of the stellar and disk orbits. For the purpose of our estimates, we set the total disk pressure as $P_{\rm tot} \sim 2.5\rho c^2 (R_{\rm g}/R)$. Equating $P_{\rm tot} = P_w$ at $R = R_{\rm p}$ gives the distance at which the stellar wind is shocked, when S2 is at pericenter:

$$r_{\rm sh} = 6 \times 10^{13} \dot{M}_{-7}^{1/2} v_8^{1/2} n_4^{-1/2} \quad \mathrm{cm}, \tag{1}$$

where $\dot{M} = 10^{-7} \dot{M}_{-7}$ $\mathrm{M_{\odot}}$ $\mathrm{yr^{-1}}$ is the stellar wind mass loss, and $n = 10^4 n_4$ $\mathrm{cm^{-3}}$ is the electron (or proton) number density of the RIAF at pericenter. Note that for reasonable parameters $r_{\rm sh} \ll R_{\rm p}$, so the wind is terminated at a “small” distance from the S2 star.

In the post-shock region, the temperature of the gas is $T_{\rm sh} = 1.3 \times 10^7 v_8^2$ K, and the electron number density is $n_{\rm sh} = 4\, n_w(r_{\rm sh}) = 3 \times 10^6\, n_4 v_8^{-2} \mathrm{cm^{-3}}$, where n_w is the electron number density in the unshocked wind. Here, we have assumed solar metallicity (our best guess for the wind from a main sequence star). The wind cools through optically thin, thermal bremsstrahlung emission. For temperatures $T \sim 10^7$K and a solar-like composition, line emission dominates the cooling rate over free-free emission by a modest factor. The emissivity is approximately constant for $T \sim (0.3 \div 3) \times 10^7$ K and of order $\Lambda_{\rm N} \sim 3 \times 10^{-23}$ erg $\mathrm{cm^3 s^{-1}}$(Stevens et al. 1992; Sutherland & Dopita 1993). The cooling timescale of the plasma is then $t_{\rm c} = 2 k_{\rm B} T_{\rm sh} / n_{\rm sh} \Lambda_{\rm N} \simeq 4 \times 10^7 v_8^4 n_4^{-1}$ s. bremsstrahlung cooling competes with the adiabatic expansion of the shocked wind. The latter takes place on a timescale $t_{\rm exp} \sim r_{\rm sh}/v_{\rm sh} \sim 4 r_{\rm sh}/v_w \simeq 2.4 \times 10^6 \dot{M}_{-7}^{1/2} v_8^{-1/2} n_4^{-1/2}$ s, where $v_{\rm sh} = v_w/4$ is the post-shock flow velocity.[1] Out of the total kinetic luminosity $L_w = \dot{M} v_w^2/2$ of the wind, a fraction $t_{\rm exp}/t_{\rm c} \simeq 0.06\, \dot{M}_{-7}^{1/2} n_4^{1/2} v_8^{-9/2}$ is radiated in the X-ray band as thermal bremsstrahlung. The X-ray luminosity of the shocked wind region is

$$L_X = \frac{t_{\rm exp}}{t_{\rm c}} L_w \sim 2 \times 10^{33} \dot{M}_{-7}^{3/2} n_4^{1/2} v_8^{-5/2} \quad \mathrm{erg\ s^{-1}}. \tag{2}$$

Given that the quiescent X-ray luminosity from Sgr A* is at a similar level (a few 10^{33} erg/s; Baganoff et al. 2003), it is possible to measure contributions to the total emission from the shocked wind when the S2 star is close to pericenter.

In Fig. 1, we present the X-ray light curves expected from the shocked wind of S2 when the star approaches its pericenter, in mid-2018. For each point along the stellar orbit – characterized by the inclination i and the argument of periapsis ω – we extract the local conditions in the disk from the model by Sadowski et al. (2013, see Table A1 there), which is based on GRMHD simulations of the accretion flow around Sgr A*.[2] We compute the shock radius $r_{\rm sh}$ at each time by balancing the wind ram pressure with the total (ram plus thermal) pressure in the accretion flow. When calculating the

---

[1] The expansion time of the shocked wind $t_{\rm exp}$ is somewhat shorter than the typical evolution time $t_{\rm ev} = R_{\rm p}/v_{\rm p}$ of the stellar orbit at pericenter (i.e., the time over which the confining disk pressure changes). We, therefore, assume that the wind-disk interface evolves quasi-steadily along the stellar orbit.

[2] The inclination i is such that $i = 0°$ if the orbital plane coincides with the disk equatorial plane. The argument of periapsis ω is measured along the orbital plane from the line of nodes, where the orbital plane intersects the disk midplane. We have $\omega = 0°$ if the pericenter is on the disk midplane.

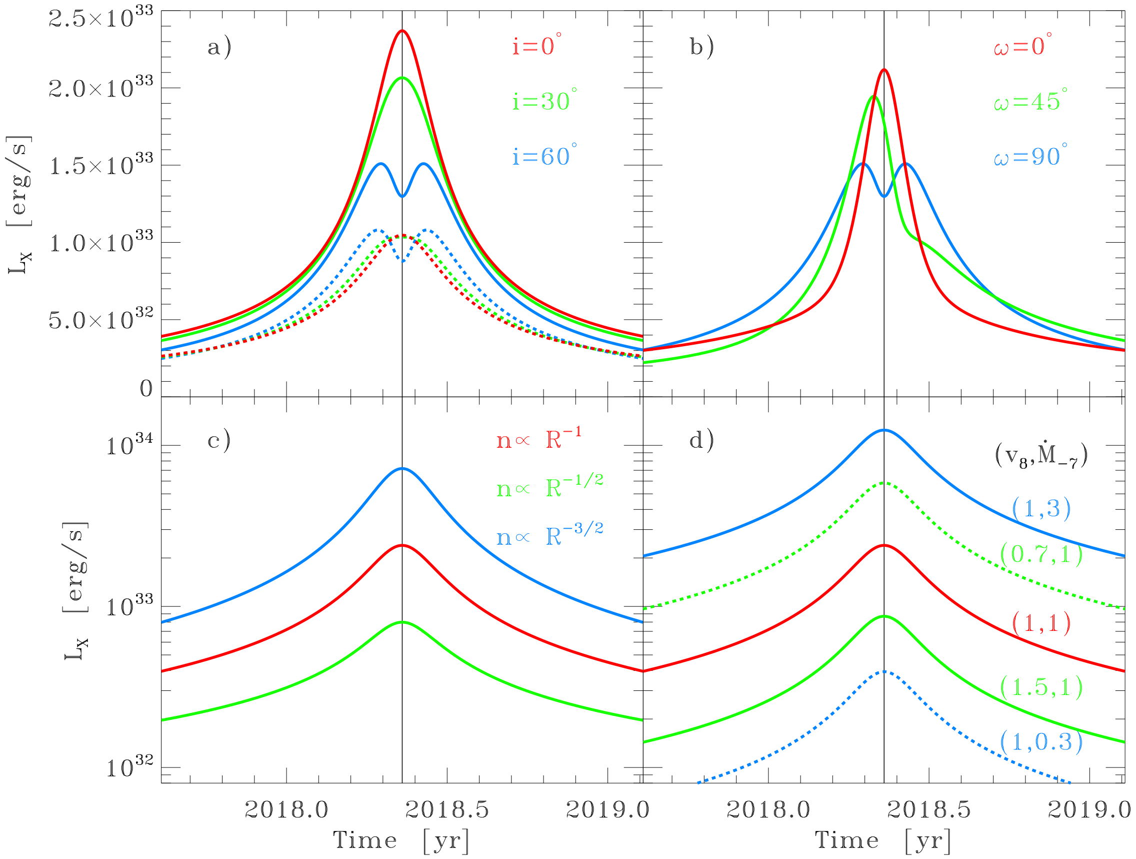

Figure 1. Lightcurves of the X-ray emission from the shocked stellar wind, for different stellar and disk parameters. In all the panels, the vertical black line marks the time of pericenter. *(a)* We vary the inclination of the stellar orbit with respect to that of the accretion disk ($i = 0°$ in red, $i = 30°$ in green, $i = 60°$ in blue), for a fixed argument of periapsis ($\omega = 90°$). Solid lines show counter-rotating orbits, dashed for co-rotating orbits. *(b)* We vary the argument of periapsis of the stellar orbit ($\omega = 0°$ in red, $\omega = 45°$ in green, $\omega = 90°$ in blue), for a fixed orbital inclination ($i = 60°$). We only show counter-rotating orbits. *(c)* We vary the density profile in the accretion flow ($n \propto R^{-1}$ in red, $n \propto R^{-1/2}$ in green, $n \propto R^{-3/2}$ in blue), for a fixed density at the Bondi radius $n_b = 130\,\mathrm{cm}^{-3}$. We only show counter-rotating orbits with $i = 0°$. *(d)* We vary the properties of the stellar wind with respect to our standard choice $(v_8, \dot{M}_{-7}) = (1, 1)$ plotted in red, by changing the wind velocity (green) or the mass loss rate (blue). We only show counter-rotating orbits with $i = 0°$.

disk ram pressure as the star moves through the disk, we differentiate between stellar orbits that are co-rotating vs counter-rotating relative to the disk azimuthal velocity. Given the shock radius $r_{\rm sh}$ at each time, we compute the X-ray luminosity as outlined above.

In panels *(a)* and *(b)*, we show how the X-ray emission depends on the orientation of the stellar orbit relative to the disk plane (we vary the inclination i in panel *(a)*, for a fixed argument of periapsis $\omega = 90°$; and we change the argument of periapsis ω in panel *(b)*, for a fixed inclination $i = 60°$). As shown in panel *(a)*, counter-rotating orbits (solid lines) always result in stronger X-ray signatures than their co-rotating counterparts (dashed lines, with the same color), since the ram pressure from the disk confines the shock closer to the star, giving a higher post-shock particle density and enhanced bremsstrahlung emission. The difference in the peak luminosity is, however, modest (at most a factor of 2) when comparing counter and co-rotating orbits. The X-ray emission peaks when the stellar orbit intersects the disk midplane, since the disk density is the highest there (and so the shock is closest to the star). Depending on the argument of periapsis, the star may cross the disk only once, at pericenter (red line in *(b)*, for $\omega = 0°$); or two times, symmetric around the pericenter epoch (blue line in *(b)*, for $\omega = 90°$); or two times, but asymmetric with respect to pericenter (green line in *(b)*, for $\omega = 45°$). The shape of the light curve around pericenter can then be used to constrain the orientation of the orbit of S2 relative to the accretion flow of Sgr A*.

The peak luminosity depends significantly on the structure of the accretion flow around Sgr A* and on the properties of the wind of S2. In panel *(c)*, we fix the disk density at the Bondi radius $n_b = 130\,\mathrm{cm}^{-3}$ and we compare the scaling $n \propto R^{-1}$ expected on the basis of GRMHD simulations (McKinney et al. 2012; Tchekhovskoy & McKinney 2012; Narayan et al. 2012; Sadowski et al. 2013) with the prediction $n \propto R^{-3/2}$ of the ADAF solution (in blue) and with the profile $n \propto R^{-1/2}$ of CDAF models (in green). In panel *(d)*, we vary the velocity and mass loss rate of the stellar wind, with respect to our reference choice $(v_8, \dot{M}_{-7}) = (1, 1)$, plotted as a red curve. The trends seen in panels *(c)* and *(d)* can be simply understood from the scalings illustrated in eq. 2, which gives the luminosity expected at pericenter. Once the properties of the stellar wind of S2 are better determined, the X-ray emission from the shocked wind could be used to place important constraints on the density profile of the accretion flow around Sgr A*.

3.2 Non-thermal radiation from the shocked RIAF

Sadowski et al. (2013) recently showed that a highly elliptical orbit of an object moving through a RIAF is likely to be supersonic for the disk itself. The Mach number of the shock is $1.5 \div 3$ depending of the relative orientation of the stellar and disk plane. The RIAF is shocked and electron acceleration has been proposed to take place at the shock front (Sadowski et al. 2013). We explore this possibility by assuming that a fraction $\epsilon \sim 0.1$ of the total dissipated energy is deposited into non-thermal electrons with a rather flat power-law energy distribution (i.e., an energy spectrum $dN/d\gamma \propto \gamma^{-2}$). Relativistic electrons will produce X-rays and γ-rays by upscattering the powerful UV radiation from the S2 star.

The RIAF material approaches the star with speed $v \sim v_{\rm p}$, dissipating kinetic energy at a rate $L_{\rm diss} \sim \pi r_{\rm sh}^2 \rho v_{\rm p}^3 \sim 10^{35} \dot{M}_{-7} v_8 {\rm erg\ s^{-1}}$. The shocked RIAF material expands on a timescale $t_{\rm exp} \sim 4 r_{\rm sh}/v_{\rm p} \simeq 3 \times 10^5 \dot{M}_{-7}^{1/2} v_8^{1/2} n_4^{-1/2}{\rm s}$. A relativistic electron with Lorentz factor γ cools on a timescale $t_{\rm c} = 3 \times 10^7/\gamma U_{\rm ph}$ s, where $U_{\rm ph} = L_*/4\pi r_{\rm sh}^2 c$ is the energy density of the stellar radiation field, and we assume that the S2 star has luminosity $L_* = 10^{38} L_{*,38} {\rm erg\ s^{-1}}$. The characteristic energy of the stellar photons is $E_* \sim 3 k_{\rm B} T_* \simeq 6\,{\rm eV}$, requiring electrons with Lorentz factor $\gamma = 70\, E_{\rm 30keV}^{1/2}$ for the production of $\sim$ 30 keV photons. A fraction $t_{\rm exp}/t_{\rm c} \simeq 0.05\, L_{*,38} E_{\rm 30keV}^{1/2} M_{-7}^{-1/2} v_8^{-1/2} n_4^{1/2}$ of the total dissipated power $L_{\rm diss}$ is radiated away. The luminosity of the IC component at photon energy E is

$$L_{\rm IC} \sim \epsilon \frac{t_{\rm exp}}{t_{\rm c}} L_{\rm diss} \sim 6 \times 10^{32} \epsilon_{-1} L_{*,38} E_{30keV}^{1/2} \dot{M}_{-7}^{1/2} v_8^{1/2} n_4^{1/2} \quad {\rm erg\ s^{-1}}. \quad (3)$$

Currently the quiescent level of emission in the hard X-rays from Sgr A* is not known. Extrapolation of the soft X-ray emission spectrum indicates that the level of hard X-ray luminosity at ~30 keV may be in the range $\sim 10^{32} \div 3 \times 10^{33}$erg/s. We conclude that $L_{\rm IC}$ may be powerful enough to be detectable in this band over the quiescent emission from Sgr A*.

Electrons with $\gamma \gtrsim 10^3 M_{-7}^{1/2} v_8^{1/2} L_{38}^{-1} n_4^{-1/2}$ are in the fast cooling regime ($t_{\rm exp}/t_{\rm cool} > 1$). As a result, all the energy that is injected in those electrons is radiated away in the form of $E \gtrsim 6\, M_{-7} v_8 L_{38}^{-2} n_4^{-1}$MeV photons. Under the optimistic assumption of a flat injection electron distribution[3] up to $\gamma \gtrsim 10^4$, as much as $L_{\rm IC} \sim 10^{34} \epsilon_{-1} \dot{M}_{-7} v_8$erg/s may be radiated in the MeV band [and up to $\sim 200\,(6\,{\rm eV}/E_*)$ GeV, where Klein-Nishina suppression appears]. Unfortunately, the high density of sources in the Galactic center region makes detecting such a γ-ray signal very challenging.

4 DISCUSSION AND CONCLUSIONS

Given its stellar type, S2 is expected to posses a moderately powerful stellar wind with $\dot{M} \sim 10^{-7} {\rm M_\odot\ yr^{-1}}$ and $v_w \sim 10^8 {\rm cm\ s^{-1}}$. Upon interaction with the accretion flow of Sgr A*, the stellar wind is shocked fairly close to the star, resulting in substantial bremsstrahlung cooling in the ~a few keV band. The predicted emission spectrum is that of optically thin, thermal bremsstrahlung, characterized by strong emission lines. The peak of the emission is predicted to take place around the pericenter passage of the star and the emission should remain bright over a several-month period (Fig. 1). The X-ray luminosity (eq. 2) is potentially detectable close to its peak (or peaks) as an increament of the quiescent emission that lasts for months[4]. The slow evolution pattern of the emission from the wind-disk interaction should allow to discriminate it from the observed rapid (minute to hours) flaring that is probably related to activity close to the black-hole horizon. The shape of the light curve around the peak(s) depends on the inclination or the orbit of S2 with respect to the disk and can be used to determine the orbital plane of the disk.

The wind-disk interaction leads to the formation of a shock in the disk material as well. If the shock of the RIAF accelerates non-thermal electrons, then IC scattering of the stellar radiation field leads to a significant hard X-ray signal. NuSTAR (Harrison et al. 2013) has the sensitivity to detect such a hard re-brightening from Sgr A* at the epoch of the pericenter passage of S2.

Similar considerations apply to the wind-disk interactions of other S stars. From eq. 2, it is clear that high wind mass loss rates, slow wind velocities and small pericenter radii result in the brightest events. However, the other members of the S cluster are dimmer than S2 and are likely to have weaker winds. For the moment S2 remains the best candidate for such a study.

The next pericenter passage of S2 will take place in 2018. By that time, a better observational understanding of the quiescent luminosity of Sgr A* may be in place in both soft and hard X-rays. This will facilitate the detection of even weak enhancements of the X-ray luminosity of Sgr A* on a timescale of months to years around the closest approach of S2. Furthermore, our work motivates the need for a more precise determination of the wind properties of S2 (such as mass loss rate, velocity and metallicity). The current limit for the wind mass loss rate from S2 is $\dot{M} \lesssim 3 \times 10^{-7} {\rm M_\odot}$ yr^{-1} (Martins et al. 2008), which is only modestly constraining. A precise assessment of the wind properties will make any detection of shocked wind emission (or even upper limits) a very powerful probe of the accretion disk.

In the Summer of 2013, the G2 cloud (Gillessen et al. 2012, 2013) is passing at its pericenter in the disk of Sgr A* at a distance of $\sim 5000\, R_{\rm g}$. Interactions of the cloud with the accretion disk may lead to X-ray (Gillessen et al. 2012) or radio (Narayan et al. 2012; Sadowski et al. 2013) signatures that can be used to probe the disk properties. An interesting fact is that the orbit of the S2 star is highly inclined with respect to that of the G2 cloud, providing a potential probe of the disk properties on a different plane.

ACKNOWLEDGMENTS

L.S. is supported by NASA through Einstein Postdoctoral Fellowship grant number PF1-120090 awarded by the Chandra X-ray Center, which is operated by the Smithsonian Astrophysical Observatory for NASA under contract NAS8-03060.

REFERENCES

Baganoff F. K., Bautz M. W., Brandt W. N., et al. 2001, Nature, 413, 45

Baganoff F. K., Maeda Y., Morris M., et al. 2003, Astrophysical Journal, 591, 891

---

[3] If the electron power-law slope is $p > 2$, the IC luminosity at a photon energy E will be suppressed by a factor of $\sim (E/E_*)^{(p-2)/2}$ with respect to the estimates given above.

[4] Current X-ray instruments do not have the angular resolution to distinguish this source from the Galactic center diffuse emission. Also the spectrum from the shocked wind is similar (within observational uncertainty) to the quiescent one from Sgr A* (Baganoff et al. 2003)

Ball G. H., Narayan R., Quataert E., 2001, Astrophysical Journal, 552, 221
Blandford R. D., Begelman M. C., 1999, Monthly Notices of the Royal Astronomical Society, 303, L1
Blandford R. D., Begelman M. C., 2004, Monthly Notices of the Royal Astronomical Society, 349, 68
Genzel R., Eisenhauer F., Gillessen S., 2010, Reviews of Modern Physics, 82, 3121
Genzel R., Schödel R., Ott T., et al. 2003, Astrophysical Journal, 594, 812
Ghez A. M., Wright S. A., Matthews K., Thompson D., Le Mignant D., Tanner A., Hornstein S. D., Morris M., Becklin E. E., Soifer B. T., 2004, Astrophysical Journal Letters, 601, L159
Gillessen S., Eisenhauer F., Fritz T. K., Bartko H., Dodds-Eden K., Pfuhl O., Ott T., Genzel R., 2009, Astrophysical Journal Letters, 707, L114
Gillessen S., Eisenhauer F., Trippe S., Alexander T., Genzel R., Martins F., Ott T., 2009, Astrophysical Journal, 692, 1075
Gillessen S., Genzel R., Fritz T. K., et al. 2012, Nature, 481, 51
Gillessen S., Genzel R., Fritz T. K., et al. 2013, Astrophysical Journal, 763, 78
Harrison F. A., Craig W. W., Christensen F. E., et al. 2013, ArXiv e-prints
Kudritzki R.-P., Puls J., 2000, Ann. Rev. Astron. Asrophys., 38, 613
Marrone D. P., Moran J. M., Zhao J.-H., Rao R., 2007, Astrophysical Journal Letters, 654, L57
Martins F., Gillessen S., Eisenhauer F., Genzel R., Ott T., Trippe S., 2008, Astrophysical Journal Letters, 672, L119
McKinney J. C., Tchekhovskoy A., Blandford R. D., 2012, Monthly Notices of the Royal Astronomical Society, 423, 3083
Mościbrodzka M., Gammie C. F., Dolence J. C., Shiokawa H., Leung P. K., 2009, Astrophysical Journal, 706, 497
Narayan R., Özel F., Sironi L., 2012, Astrophysical Journal Letters, 757, L20
Narayan R., Sädowski A., Penna R. F., Kulkarni A. K., 2012, Monthly Notices of the Royal Astronomical Society, 426, 3241
Narayan R., Yi I., Mahadevan R., 1995, Nature, 374, 623
Quataert E., Gruzinov A., 2000, Astrophysical Journal, 539, 809
Sadowski A., Sironi L., Abarca D., Guo X., Ozel F., Narayan R., 2013, ArXiv e-prints
Stevens I. R., Blondin J. M., Pollock A. M. T., 1992, Astrophysical Journal, 386, 265
Sutherland R. S., Dopita M. A., 1993, Astrophysical Journal Suppl. Ser., 88, 253
Tchekhovskoy A., McKinney J. C., 2012, Monthly Notices of the Royal Astronomical Society, 423, L55
Yuan F., Quataert E., Narayan R., 2003, Astrophysical Journal, 598, 301